Acta Oceanol. Sin., 2024, Vol. 43, No. 1, P. 99–111
https://doi.org/10.1007/s13131-023-2230-6
http://www.aosocean.com
E-mail: ocean2@hyxb.org.cn

Research on the generation method of seawater sound velocity model based on Perlin noise

Zhimiao Chang[1], Fuxing Han[1], Zhangqing Sun[1]*, Zhenghui Gao[1], Xueqiu Wang[1]

[1] College of Geoexploration Science and Technology, Jilin University, Changchun 130026, China

Received 4 April 2023; accepted 20 June 2023

Abstract

In the processing of conventional marine seismic data, seawater is often assumed to have a constant velocity model. However, due to static pressure, temperature difference and other factors, random disturbances may often frequently in seawater bodies. The impact of such disturbances on data processing results is a topic of theoretical research. Since seawater sound velocity is a difficult physical quantity to measure, there is a need for a method that can generate models conforming to seawater characteristics. This article will combine the Munk model and Perlin noise to propose a two-dimensional dynamic seawater sound velocity model generation method, a method that can generate a dynamic, continuous, random seawater sound velocity model with some regularity at large scales. Moreover, the paper discusses the influence of the inhomogeneity characteristics of seawater on wave field propagation and imaging. The results show that the seawater sound velocity model with random disturbance will have a significant influence on the wave field simulation and imaging results.

Key words: Munk model, Perlin noise, seawater inhomogeneity

Citation: Chang Zhimiao, Han Fuxing, Sun Zhangqing, Gao Zhenghui, Wang Xueqiu. 2024. Research on the generation method of seawater sound velocity model based on Perlin noise. Acta Oceanologica Sinica, 43(1): 99–111, doi: 10.1007/s13131-023-2230-6

1 Introduction

In marine seismic exploration, seawater is commonly considered as a static or constant velocity "geological body" for data collection. However, this assumption does not account for the impact of physical factors, such as temperature and pressure, which cause the seawater velocity to vary with time. Additionally, multiple observations made at the same location to suppress multiple waves can distort and disturb the seismic rays in the seawater, altering the propagation path and affecting the processing results of seismic data (Wei, 2021; MacKay et al., 2003; da Silva Ritter, 2010). Due to the difficulty in accurately measuring seawater sound velocity, it is necessary to develop a method for generating a seawater sound velocity model to study various wave fields in the presence of seawater inhomogeneity.

When using wave equation or seismic ray method for forward modeling, generally, the generation of forward model is carried out by hand-drawing (Wang et al., 2020, 2021). When it is necessary to study the randomness and stratification of the formation, a special model generation method is required. At present, random medium model theory is often used for model generation in land seismic forward modeling. This method is mainly based on statistical principles to describe inhomogeneity stratigraphic models, and uses autocorrelation functions to constrain their random distribution (Xi and Yao, 2001; Ikelle et al., 1993). Many scholars have conducted forward modeling simulations and analyzed the seismic wavefield response characteristics of random media models (Korn, 1993; Holliger and Levander, 1994; Holliger et al., 1994). These studies have also demonstrated that small perturbations within the medium can have a significant impact on the seismic wavefield characteristics (Xi and Yao, 2001; Yong et al., 2021). However, for the forward modeling of marine seismic exploration, because seawater has completely different properties from land, such as dynamics, the stochastic medium model theory cannot fully simulate the characteristics of seawater, and a new method is needed to generate the seawater sound velocity model.

The Munk model was originally proposed by Walter H Munk in 1974 (Munk, 1974), which is a method for simulating sound velocity profiles using mathematical methods, and the resulting equations are empirical equations. In general, to know the velocity parameters of seawater at a certain position, information such as pressure, temperature, salinity, etc. are required. But the Munk model is designed to collect only parameters such as depth. Since pressure, temperature, salinity and other information are often not collected in marine seismic exploration, the Munk model is very suitable for solving problems related to seawater sound velocity in marine seismic exploration (Sun, 2021). Some scholars have also conducted research on the characteristics of the acoustic wave field in the case of the deep sea channel (Han et al., 2015). The Munk model, however, only describes the vertical changes of the seawater with varying depth, but it fails to describe the horizontal changes. Therefore, only using the Munk model for seawater sound velocity modeling will have certain limitations. In order to make the seawater sound velocity expressed by the Munk model also have a certain random variation in the horizontal direction, Qi (2015) superimposed random noise on the Munk model for wave field forward modeling. However, this method destroys the second-order continuity of the original model, and also has limitations. Therefore, this article considers using the second-order continuous Perlin noise for superposition to add more continuity to the generated seawater sound velocity model.

Foundation item: The General Program of National Natural Science Foundation of China under contract No. 42074150.
*Corresponding author, E-mail: sun_zhangq@jlu.edu.cn

Perlin noise is a noise generation method in the field of computer graphics. In the 1980s, in order to improve the shortcomings of the discontinuous gradient of white noise, Perlin (1985) used the gradient grid as the basis to generate first-order continuous random noise. In 2002, he improved this method by adding second-order continuity to Perlin noise. Because the Perlin noise is simple to generate and easy to expand, it was quickly applied to film and animation production after it was proposed. Another characteristic of Perlin noise is that it is easy to dynamize. By rotating the gradient, the Perlin noise can show a dynamic and continuous characteristic, which is consistent with the dynamic characteristics of seawater expected in this article.

Based on the issues mentioned above regarding the scarcity of seismic data or forward models for inhomogeneous seawater conditions, this paper presents a method for generating a dynamic seawater sound velocity model that incorporates the Munk model and second-order continuous Perlin noise. The proposed approach enables the seawater sound velocity model to exhibit desirable features such as continuity, randomness, dynamics, and regularity at a macroscopic scale. This approach can provide a more diverse theoretical model for theoretical research. Furthermore, this study investigates the impact of seawater inhomogeneity on wave field propagation and imaging, providing valuable insights into the field of marine seismic exploration.

2 Basic theory

2.1 *Perlin noise*

In early film and television animation production, when people want to show some random phenomena, they often achieve it through random white noise. When we observe randomly undulating mountains, endless rivers, randomly distributed hills, such randomness tends to be regular and continuous. But if we run random simulations with white noise, the results will be inappropriate. As shown in Fig. 1, Fig. 1a shows random white noise and Fig. 1b shows continuous Perlin noise. Obviously, most natural phenomena fit Fig. 1b rather than Fig. 1a.

The generation method of Perlin noise is shown in Fig. 2.

Divide the calculation area A into two sets of grids: the calculation grid and the gradient grid. The calculation grid is the storage location of each random number; the gradient grid is the basis for generating random numbers. As shown in Fig. 2, in the 5×5 grid, the red line is marked as the gradient grid, and a gradient direction and size are randomly generated at each gradient point. For the random number at the calculation point, the calculation can be performed according to the vector corresponding to the calculation point to the nearest four gradient points and the gradient on the gradient point.

As shown in Fig. 3, for the Perlin noise value of point P, the calculation method is as follows.

First calculate the respective vector dot products:

$$\begin{cases} TA = A \cdot AP, \\ TB = B \cdot BP, \\ TC = C \cdot CP, \\ TD = D \cdot DP. \end{cases} \tag{1}$$

"Smooth" the above three results as the value of point P:

$$\begin{cases} l_1 = TA + (TB - TA) \times fade(x_P), \\ l_2 = TC + (TD - TC) \times fade(x_P), \\ u_P = l_1 + (l_2 - l_1) \times fade(z_P). \end{cases} \tag{2}$$

where, u_P is the generated random value of point P, where $fade\,(x)$ is a smoothing function. TA, TB, TC, TD, l_1 and l_2 were in-

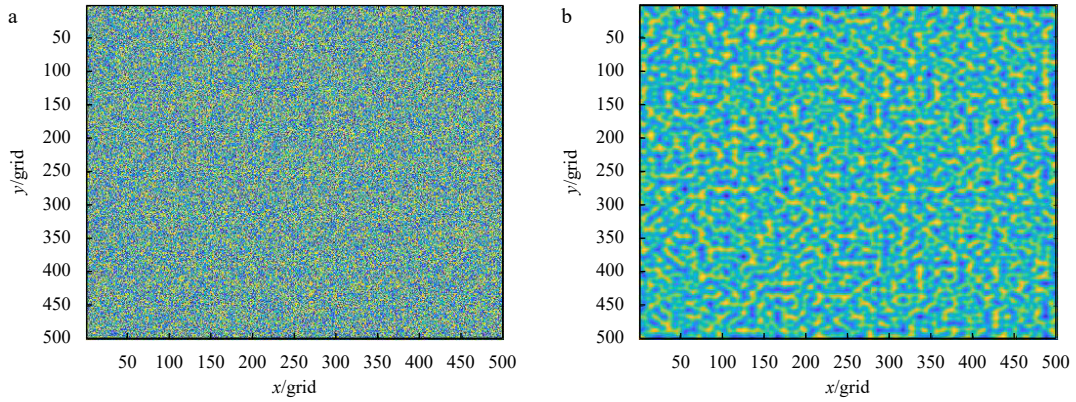

Fig. 1. Random white noise (a) and Perlin noise (b).

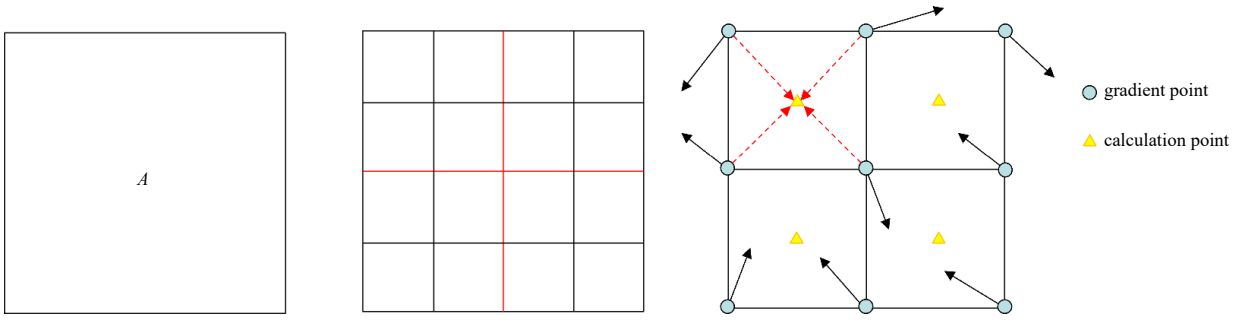

Fig. 2. Schematic diagram of Perlin noise generation.

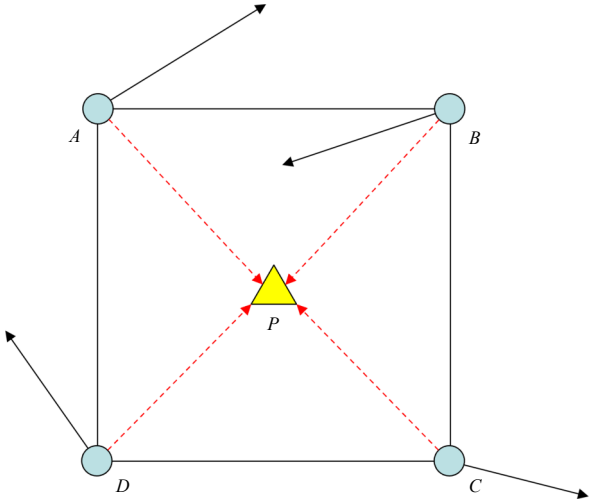

Fig. 3. Schematic diagram of gradient calculation.

termediate variables.

During the calculation, the smoothing function used is

$$fade\,(t) = 6t^5 - 15t^4 + 10t^3, \tag{3}$$

where t is the amount that needs to be smoothed.

Since seawater is dynamic all the time, there needs to be a way to convert Perlin noise to something dynamic. The method used in this article is to rotate the gradient direction, as shown in Fig. 4.

When the rotation rate is determined, the noise distribution at the new time is determined according to the new gradient direction, so that the overall Perlin noise can be guaranteed to be dynamic at all times. Under the grid of 500 × 500, the generation effect is shown in Fig. 5.

It can be seen from the figure that in the static case, Perlin noise can well demonstrate the "continuity". Unlike random white noise, every point of Perlin noise is theoretically second-order derivative. Figure 5a is the Perlin noise distribution map of four moments with a gradient grid size of 10 × 10; Fig. 5b is a Perlin noise distribution map of four moments with a gradient grid size of 20 × 20. Comparing Figs 5a and b, it can be seen that as the gradient grid becomes denser, the noise will change more drastically with the position (that is, the frequency of noise changes in the same size area is faster). The Fig. 5c, is designed to show that Perlin noise can also generate continuous noise distributions with fractal properties. If the seawater sound velocity distribution is considered to have fractal characteristics, then different gradient grids, that is, the superposition of noise distributions at different scales, can be used to generate similar noise distributions at different scales. Under the dynamic effect, the noise distribution changes smoothly at each moment, and there is no sudden change in the time dimension. In this case, it is much more convenient to calculate the travel time and ray path, and it also convenient for the subsequent discussion on the inhomogeneity characteristics of seawater sound velocity.

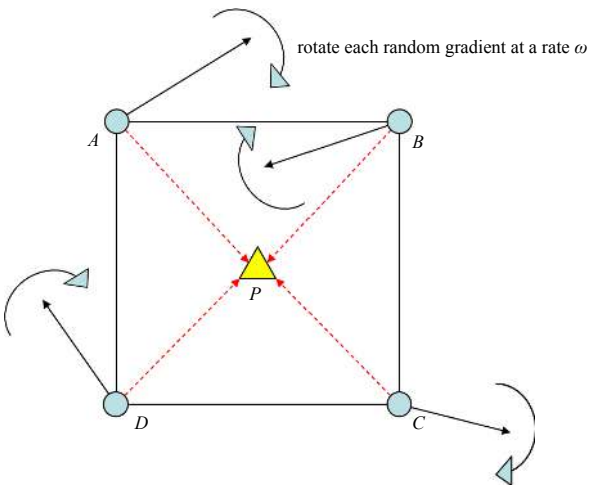

Fig. 4. Schematic diagram of gradient direction rotation.

Compared with the random medium modeling method used by other scholars in their numerical simulations, the method of using Perlin noise to generate seawater background disturbance has two main advantages. One is that Perlin noise has a simpler calculation form. Compared with the random medium modeling method, Perlin noise does not need to be operated on the spectrum, but only needs to be interpolated in the space domain, which is easier to implement on a computer. The second is that Perlin noise can easily generate time-discrete dynamic noise by means of rotating gradients, while random medium modeling methods do not have advantages in generating dynamic background disturbances.

2.2 *Munk model*

The mathematical form of the Munk model is

$$v\,(z) = v_0\{1 + \varepsilon[\mathrm{e}^{-\eta} - (1-\eta)\,]\}\,. \tag{4}$$

In the formula, v_0 is the velocity at the channel axis; $\varepsilon = \dfrac{W\gamma_{\mathrm{A}}}{2}$, where W is the channel width, γ_{A} is the adiabatic velocity gradient, and the general value is $\gamma_{\mathrm{A}} = 0.011\,4\ \mathrm{km}^{-1}$; $\eta = \dfrac{2(z-z_1)}{W}$, where z is the computed depth and z_1 is the channel axis depth.

In the case of a 500 × 500 grid (grid width is 10 m), the parameters are set to $v_0 = 1\,500$ m/s, $W = z_1 = 1\,000$ m, the simulation effect is as shown in the Fig. 6.

Under the constraints of the formula, the generated seawater sound velocity model can show the deep-sea channel phenomenon, which is similar to the actual situation. However, in practice, the seawater sound velocity changes not only vertically with depth, but also in the horizontal direction. In the actual seawater medium, it is not exactly as described by the Munk model. The seawater medium is a heterogeneous medium. Seawater is filled with a large number of suspended particles, bubbles, aerosols and other substances. Compared with seawater, these substances have a small scale, so the seawater has small-scale heterogeneity. These substances are widely distributed, and have certain randomness and dynamics. Therefore, when sound waves propagate in seawater, affected by these substances, the speed of sound waves varies from place to place. Only using the Munk model to describe the seawater acoustic wave velocity model cannot show the randomness and dynamics at the relatively small scale mentioned above, so the Munk model has certain disadvantages.

3 Model building process

As shown in Fig. 7, the generation of the model is mainly divided into the following steps.

Step 1: Perform grid planning, that is, distinguish between gradient grids and computational grids.

Step 2: Generate random gradients on the planned gradient grid.

a. Perlin noise at 4 moments when the gradient grid is 10 × 10

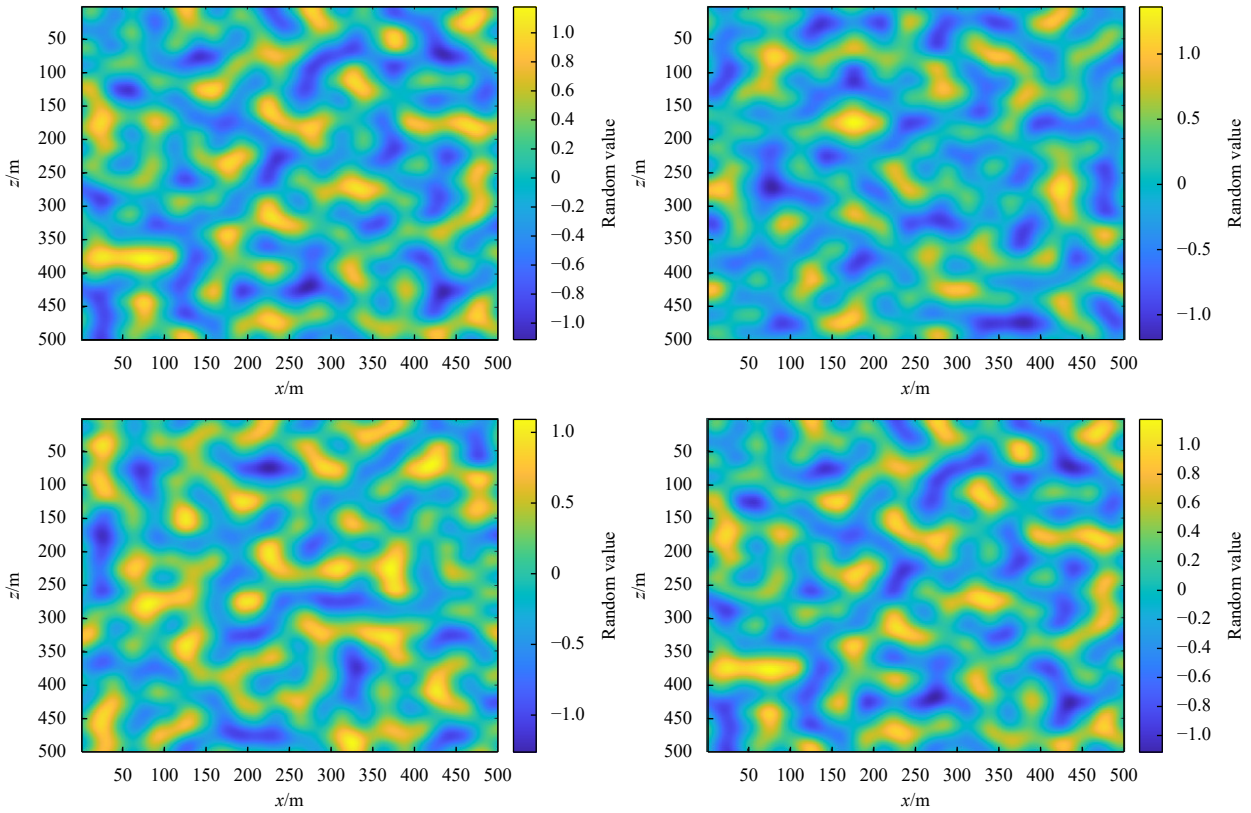

b. Perlin noise at 4 moments when the gradient grid is 20 × 20

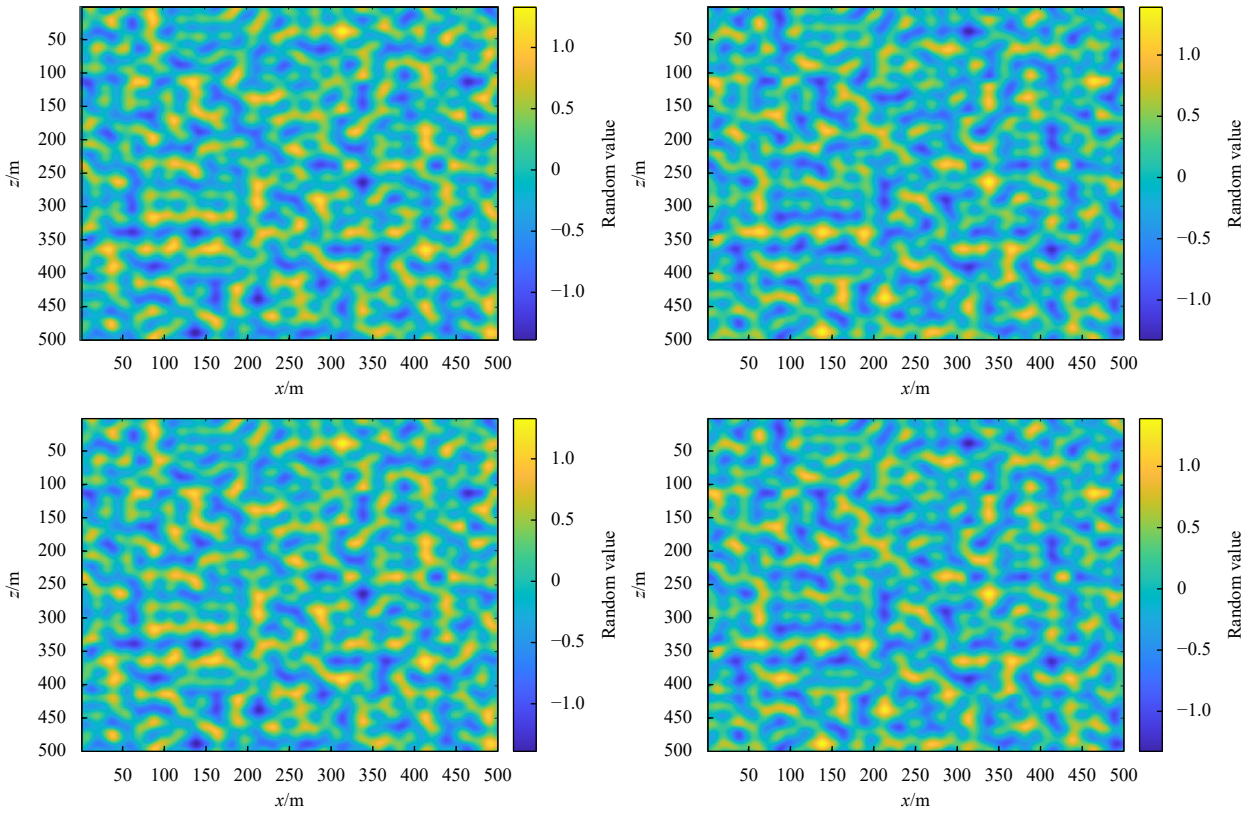

Fig. 5.

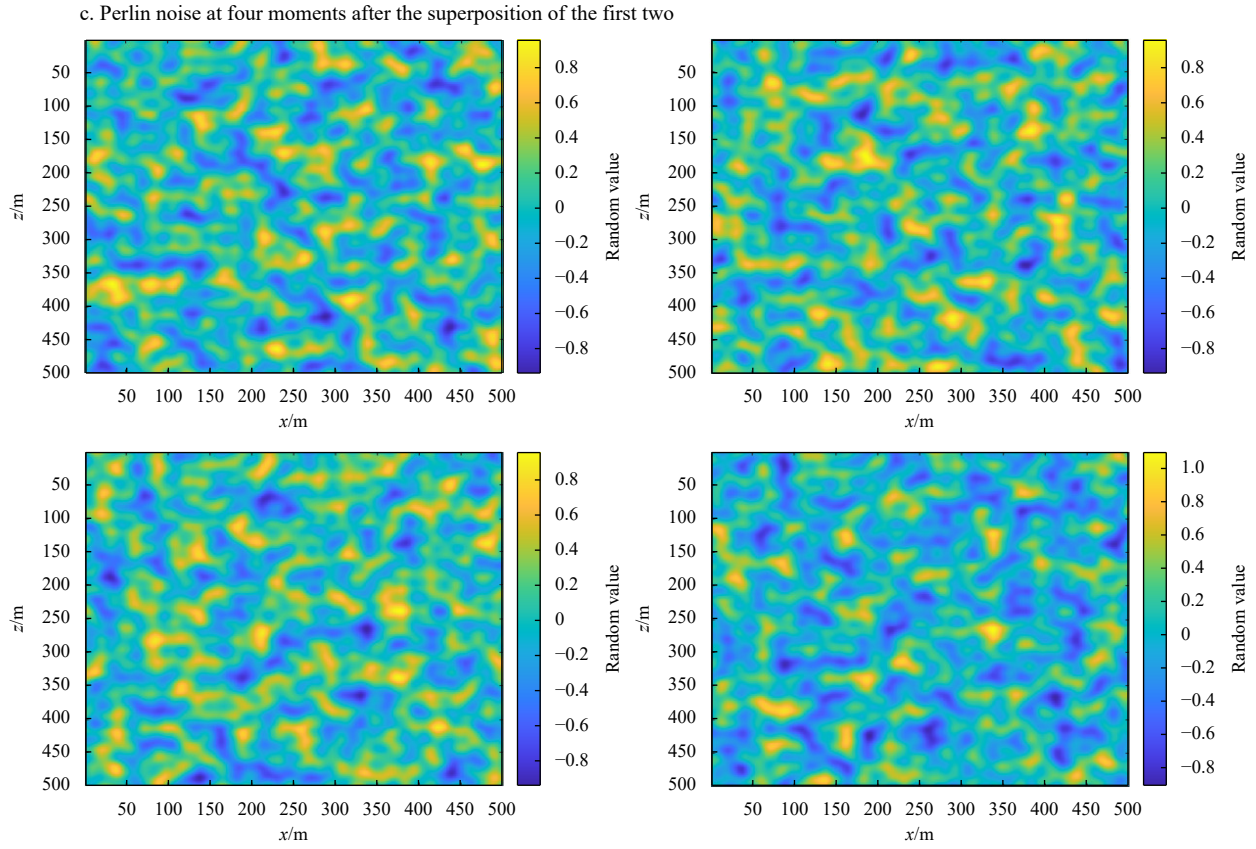

Fig. 5. Perlin noise generation effect.

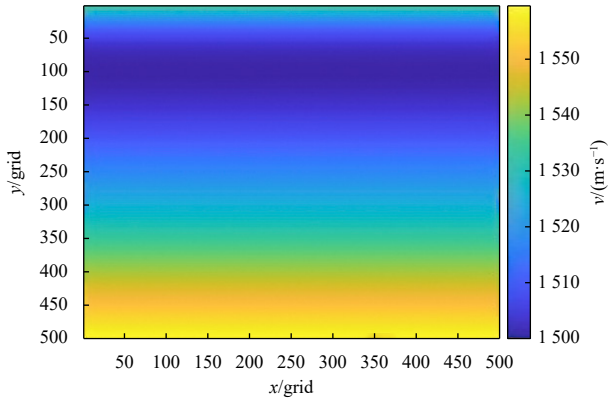

Fig. 6. Sound speed simulation effect of Munk model.

Step 3: Calculate the corresponding dot product of each calculation grid point according to the distribution of the random gradient.

Step 4: According to the calculated dot product, smooth the point and calculate the random value of the point.

Step 5: For the next point, repeat Step 3 and Step 4 until all points on the entire computational grid are traversed.

Step 6: If you want to calculate the dynamic model, you need to rotate the random gradient generated in Step 2, and repeat Step 3–Step 5.

Step 7: According to the computational grid size, generate the Munk model and sum it with the previous noise distribution.

Step 8: Output the static/dynamic random seawater sound velocity model.

In the model generated this time, the grid size is 500 × 500, and the grid spacing is 10 m. In the following discussion, if the grid spacing has no unit, it represents the number of grid points in the interval. The parameters of the Munk model are set as $v_0 = 1\,500$ m/s, $W = z_1 = 1\,000$ m.

The model integrating the Munk model and Perlin noise can also guarantee at least second-order continuity as either of them can guarantee at least second-order continuity. For static models, as shown in Fig. 8, whether it is wave field calculation, travel time calculation or ray calculation has certain advantages. In addition, since both define the speed points on the grid, they can also fit well with the undulating sea surface.

The seawater sound velocity has the characteristics of random distribution on both large and small scales, so the use of multiple grids to superimpose can better demonstrate this property. In this article, the above two superposition methods are used as examples to generate the two models shown in Fig. 9. For Fig. 9a, using a larger gradient grid can show a large-scale random distribution of velocity; Fig. 9b shows a small-scale variation of seawater sound velocity. Different generation methods can explore different scientific problems, and can also generate models according to different sea conditions.

4 Influence and analysis of heterogeneous seawater on seismic travel time, ray path and imaging

4.1 *Seismic wave travel time analysis under inhomogeneity seawater sound velocity model*

In order to demonstrate the usability of the model and the effect of random seawater sound velocity on the travel time, this paper conducts a travel time calculation experiment on the static model. The size of the model used in this paper is 500 × 500, the

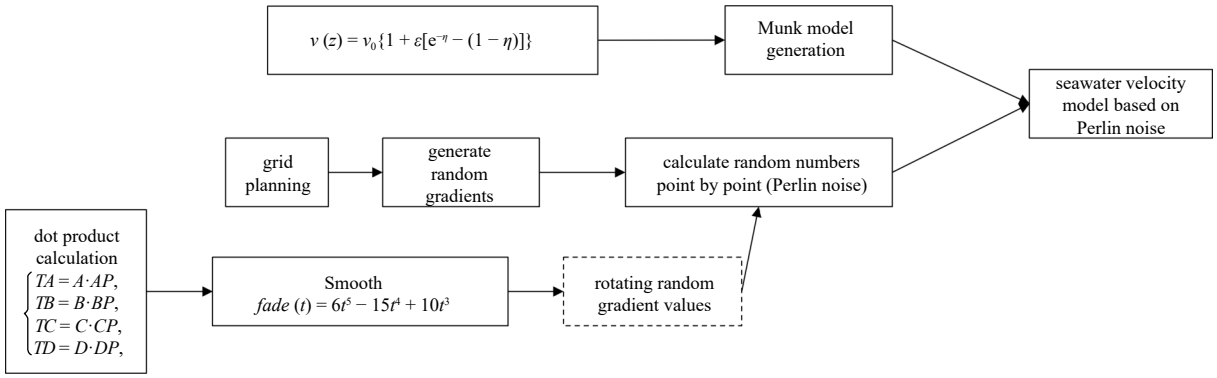

Fig. 7. Model building process.

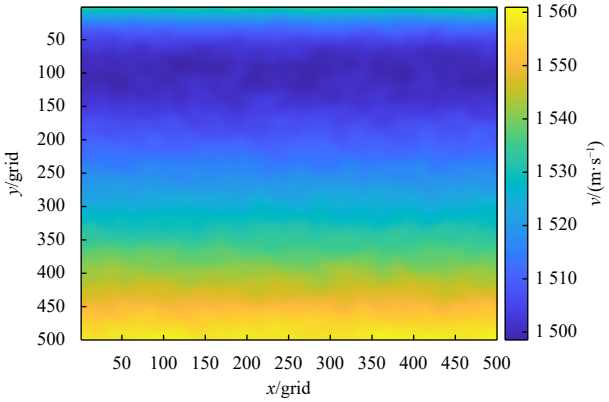

Fig. 8. Random seawater sound velocity model result under static condition.

grid spacing is 10 m, and the distribution of Perlin noise in it is [–10, 10]. The parameters of the Munk model are $v_0 = 1\ 500$ m/s, $W = z_1 = 1\ 000$ m. The model settings are shown in Fig. 10.

The hypocenter position is set at (250, 20), and the travel time distribution of the two calculated by the Fast Marching Method (Sun et al., 2017) is shown in Fig. 11.

The absolute errors of the two are shown in Fig. 12.

The distribution of absolute errors has certain randomness. Compared with the speed of seawater, the sound wave in seawater travels several kilometers per second, so the change caused by this speed disturbance is less than 1%, and this change also brings a higher error. For example, in Fig. 12 the lower left and lower right areas, the travel time error is between 0.020 and 0.025. If it is converted into distance, the error will come to about 30 m. The above discussions are all carried out in seawater, and Fig. 13 considers the error of travel time in the presence of strata.

Figure 13 adds 300 m of media with a velocity of 3 000 m/s under seawater. The error distribution of the travel time is similar to the above. In the stratigraphic part, it can be clearly seen that the travel time of the two models produces a large error at the same position. There is a similar manifestation in the absolute error. As shown in Fig. 13c, the minimum of the absolute error is above 0.025 s, because of the 3 000 m/s's media, it can be converted into distance, the error will come to about 75 m.

4.2 *Numerical simulation and discussion of underwater ray paths in inhomogeneous seawater*

In order to demonstrate the usability of the model and the effect of random seawater sound velocity on the ray path, this paper conducts ray path calculation experiments for static and dynamic models. The selected static model is shown in Fig. 10, and the dynamic model is shown in Fig. 14, where the Munk model parameters are: $v_0 = 1\ 500$ m/s, $W = z_1 = 1\ 000$ m. The random offset of Perlin noise uses a gradient grid of 10×10 and 50×50, and rotates the gradient direction at a speed of (pi/75) rad per second.

Figure 14 shows the seawater sound velocity model at four times. Compared with the static model in Fig. 10, the dynamic model in Fig. 14 not only achieves random effects in space, but also achieves random changes in time scales. The next step is to perform ray tracing experiments on the model shown in Fig. 10 and the model shown in Fig. 4.

Firstly, the travel time calculation test is carried out for the Munk model with no random offset, the random seawater model with a deviation range of [–1, 1], and a random seawater sound velocity model with a deviation range of [–10, 10]. The results obtained are shown in Fig. 15 and Fig. 16.

It can be seen from the comparison results that for the static model, when the random deviation is small, it has little effect on the travel time results. However, when the deviation increases, the impact on the ray path will become larger and larger. Finally, for the rays emitted from the same angle, the final position may deviate from the original position by more than 50 m (in the case of seawater at a depth of 5 000 m).

For the dynamic seawater random velocity model, the travel time results are shown in Fig. 17.

The calculation results in Fig. 17 were performed with a random deviation of [–1, 1]. The dynamic random seawater in this case does not change the results much compared to the static seawater sound velocity model. The ray paths have changed slightly. The ray paths below the red dividing line have changed slightly, but the ray paths have not changed much. On the whole, the longer the forward distance of the ray, the greater the difference between the ray paths under the static model and the dynamic model.

Figure 18 is a random seawater sound velocity model with deviation in the range of [–10, 10].

In Fig. 18c, it can be seen that in the area below the red dividing line, the rays of static seawater and dynamic seawater deviate significantly (the red ray representing dynamic sea depth and the blue ray representing static sea depth no longer overlap). This means that when we study the seismic forward and inversion in the deep sea, we must overcome the problem of seismic propagation path distortion caused by dynamic seawater from the perspective of accuracy.

Next, we discuss the effect of random seawater medium on the ray path of the seabed formation. The model used above was changed to replace the medium below 3 000 m with a static me-

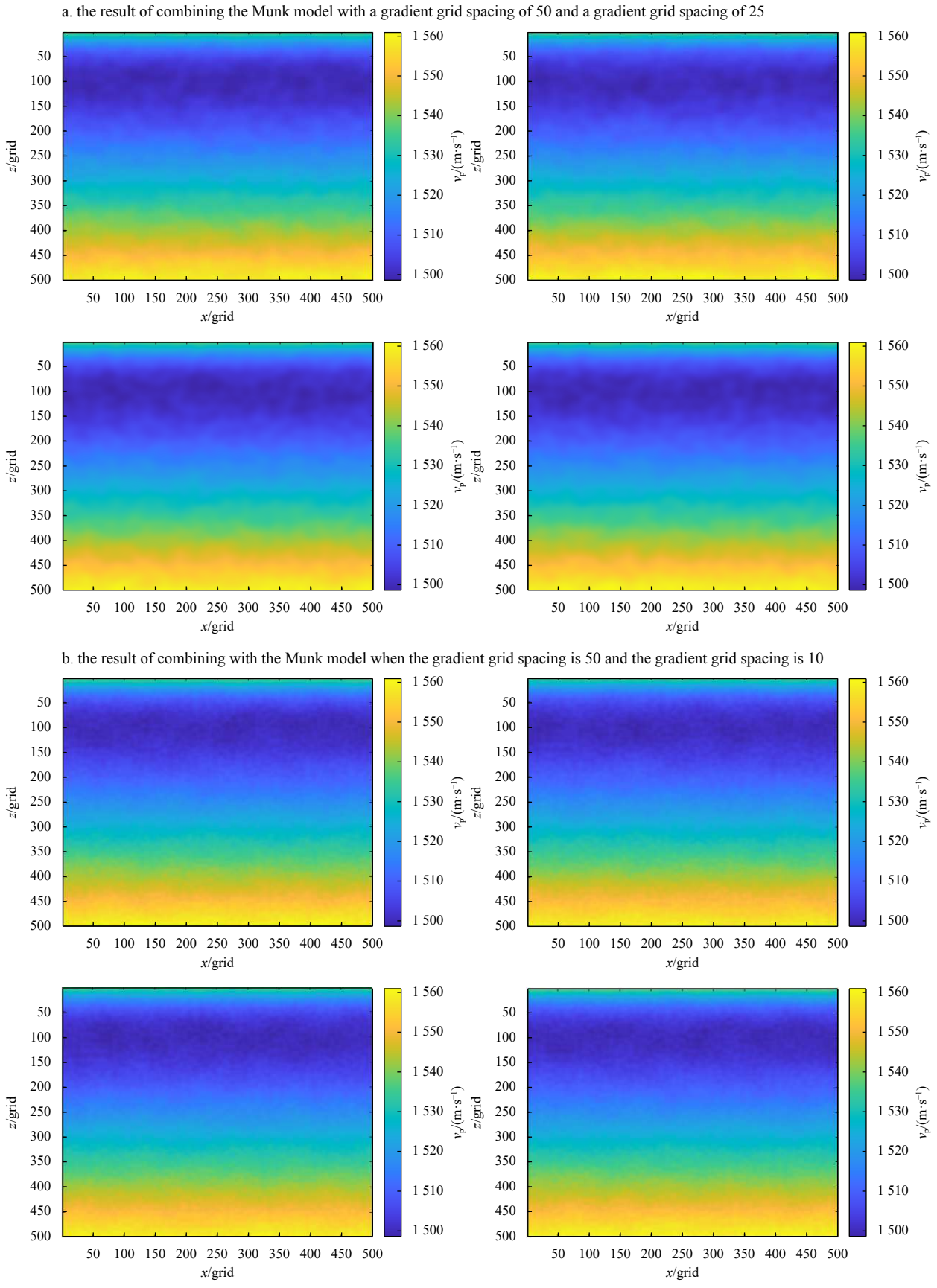

Fig. 9. Random seawater sound velocity model result under dynamic conditions (from top left to bottom right figure means the speed distribution for four consecutive times for a and b respectively). v_p means primary wave velocity.

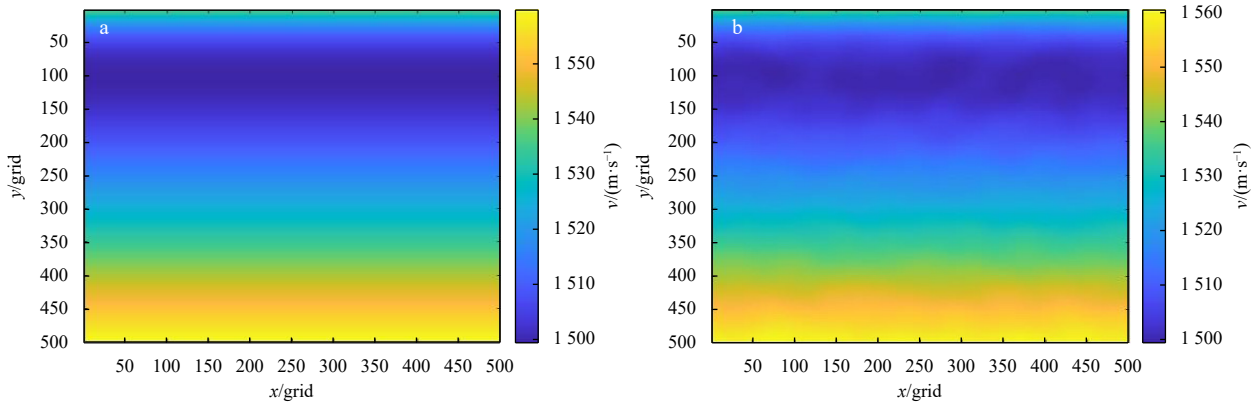

Fig. 10. Munk model result and random seawater sound velocity model result. a. Munk model without Perlin noise; b. random seawater sound velocity model with Perlin noise superimposed.

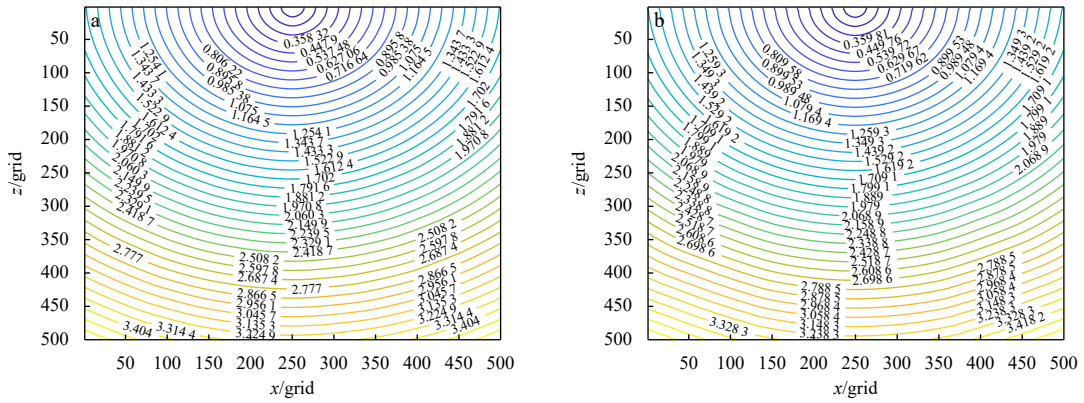

Fig. 11. Travel time distribution diagram. a. Travel time diagram of Munk model; b. travel time diagram of random seawater sound velocity model.

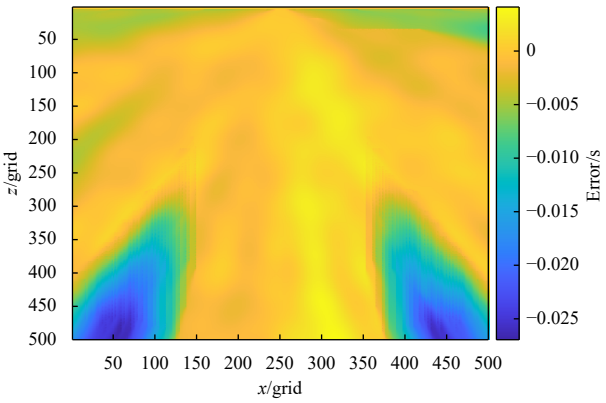

Fig. 12. Travel time absolute error.

dium with a velocity of 1 800 m/s. The result is shown in Fig. 19.

It can be seen that the dynamic seawater has a great influence on the ray path in the seabed formation. Even in the seawater layer, when the static and dynamic paths are not much different, the propagation directions of the two will be changed by the dynamic seawater. In the formation, the part below $z = 300$, the propagation path is greatly deviated.

The above is the discussion of travel time calculation for simple models, then for complex models, the problem of whether the ray path deviates will be magnified, which is a problem worthy of study.

The travel time calculation results for the complex model in this paper are shown in Fig. 20.

In this model, the depth within 3 000 m is set as seawater, and the rest is static formation medium. The seawater medium is set as dynamic and static, respectively, and a comparative calculation is carried out. The Perlin noise perturbation employed by both models is [–1, 1].

It can be seen from the figure that although the seawater layer accounts for about 19% of the entire model, it still has a great influence on the deep medium. In Fig. 20c, it can be seen that the red and blue rays are almost completely misaligned as the rays propagate forward. However, the effect is mainly for the change of the ray along the longitudinal direction, and the change of the component along the transverse direction of the ray propagation is limited. This result shows that the influence of the randomness of seawater on the ray path must be considered when conducting deep-sea seismic exploration.

4.3 *Imaging features of inhomogeneity seawater*

The most direct effect of the distortion of the ray path shown in Fig. 20 is the imaging effect. This section will take the Gaussian beam imaging method as an example to explore the influence of static random seawater in the imaging process. The imaging effects under the horizontal layer model, the undulation model and the complex model are discussed respectively.

The horizontal layer model is shown in Fig. 21.

The above three models are used as the ray solution basis for Gaussian beam imaging (the smoothing times of the model are fixed at 100 times), and the random disturbance model of seawa-

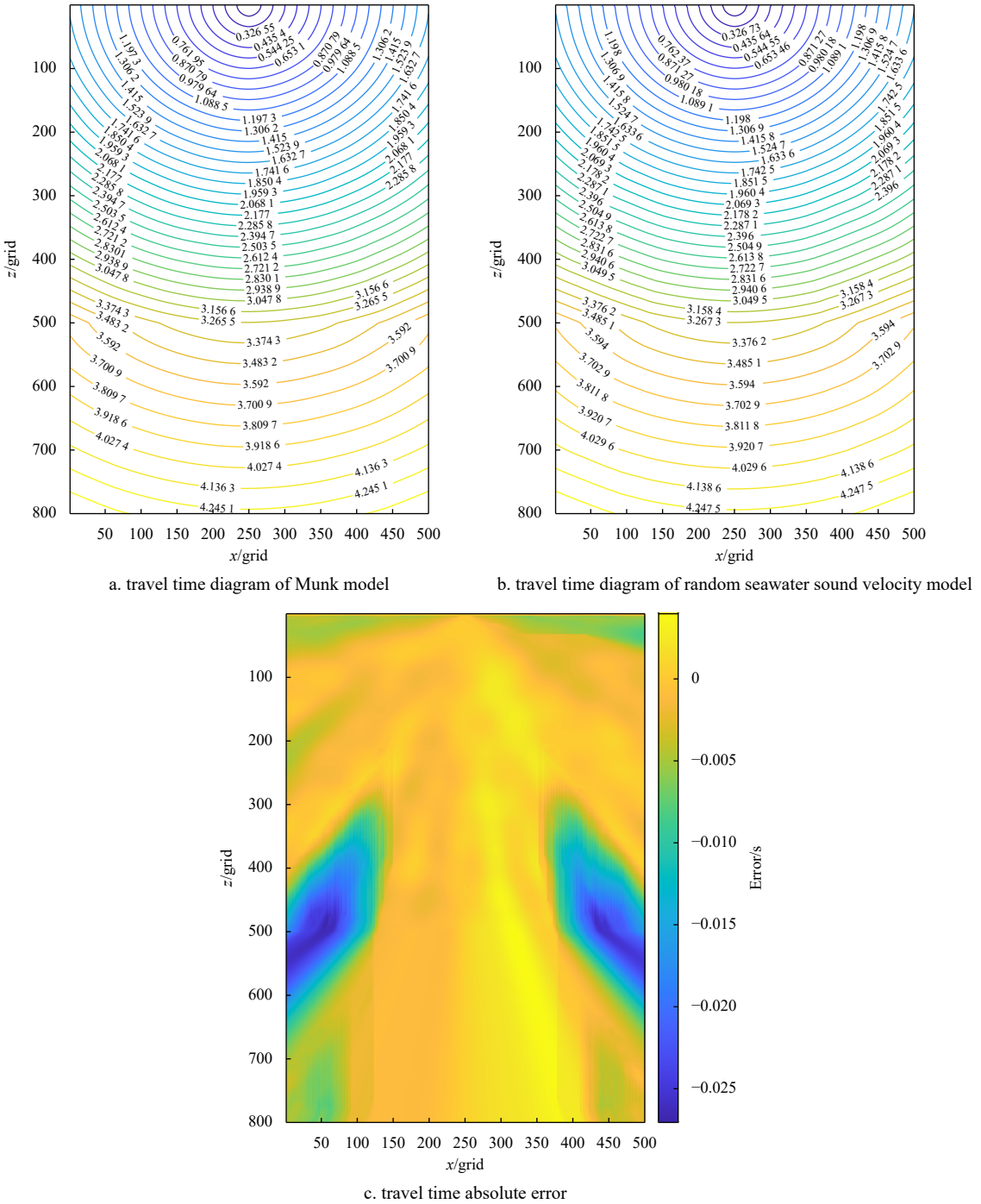

a. travel time diagram of Munk model

b. travel time diagram of random seawater sound velocity model

c. travel time absolute error

Fig. 13. Travel time and its absolute error after adding strata.

ter layer is used as the basis for the simulation of seismic records, and the Gaussian beam imaging experiment is carried out. The final result is shown in Fig. 22.

Compared with the other two, the imaging results of the constant velocity seawater layer have a certain deviation in the horizon, and the energy is relatively deconcentrated on the event axis, which may be caused by random factors in the seismic records. For the imaging results of using the Munk model as the seawater layer, its energy is relatively concentrated. For the results of Gaussian beam imaging using the random seawater sound velocity model, further irregularities are exhibited in the event axis. Moreover, due to the instability of the ray path, there will be a lot of data similar to “random noise” near the offset horizon.

For the undulation model, the model is shown in Fig. 23.

The Gaussian beam imaging parameters are the same as the former, and the final imaging result is shown in the Fig. 24.

The results under the constant velocity model still exits horizon upshift. For the second horizon, due to random disturbance, the imaging effect is not good, and distortion and bending also occur. At the same time, there is also energy discontinuity in the undulating horizon. These phenomena are caused by inhomogeneity seawater sound velocity.

For complex models, the model is shown in Fig. 25.

The Gaussian beam imaging parameters are the same as the former, and the final imaging result is shown in the Fig. 26.

In the case of complex models, the imaging results produce

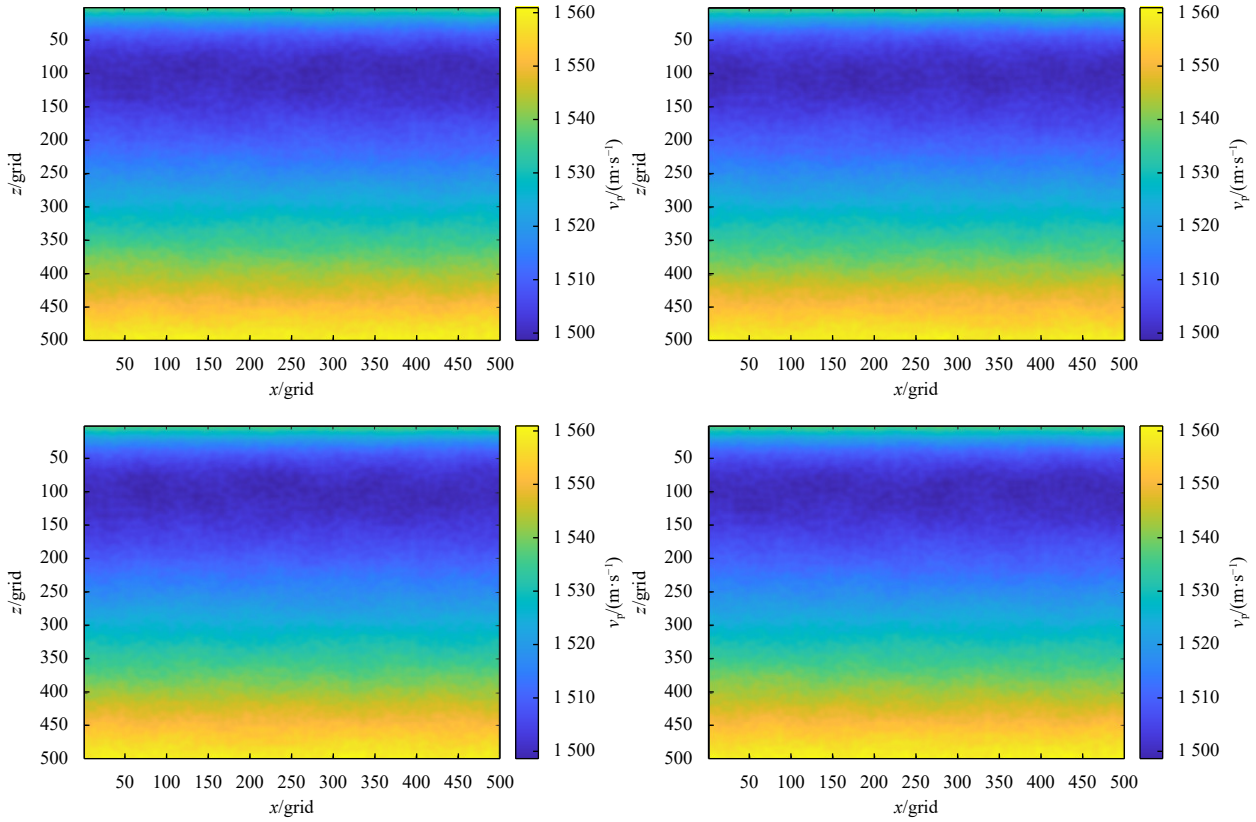

Fig. 14. Random seawater sound velocity model result under dynamic conditions (the results of four moments combined with the Munk model when the gradient grid spacing is 50 and the gradient grid spacing is 10). v_p means primary wave velocity.

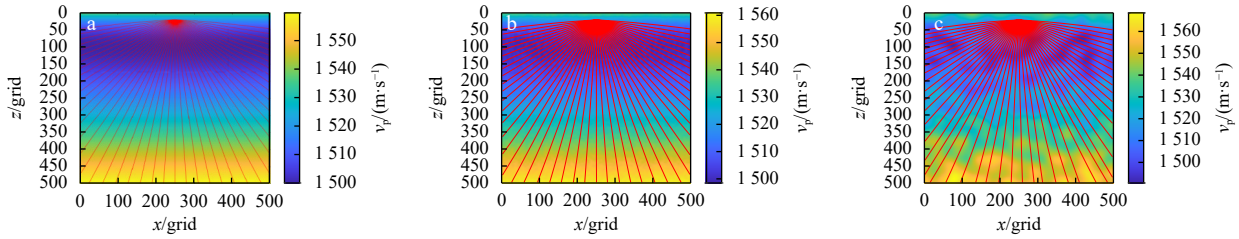

Fig. 15. Calculation results of ray path. a. The calculation results of the ray path of the Munk model without random offset; b. the calculation results of the ray path of the random seawater model with a deviation range of [–1, 1]; c. the calculation results of the ray path of the random seawater sound velocity model with a deviation range of [–10, 10]. v_p means primary wave velocity.

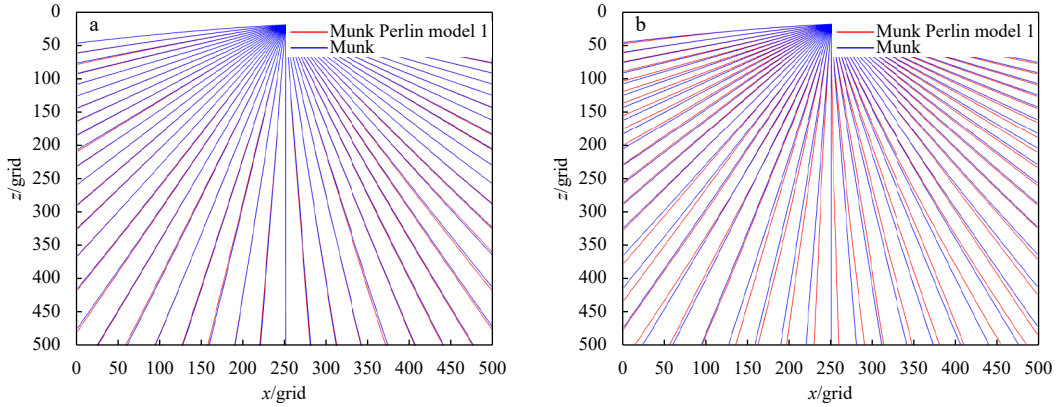

Fig. 16. Comparison of ray path results. a. Comparison of the ray path results of the Munk model without random deviation and the random seawater model with a deviation range of [–1, 1]; b. comparison of the ray path results of the Munk model without random deviation and the random seawater model with a deviation range of [–10, 10].

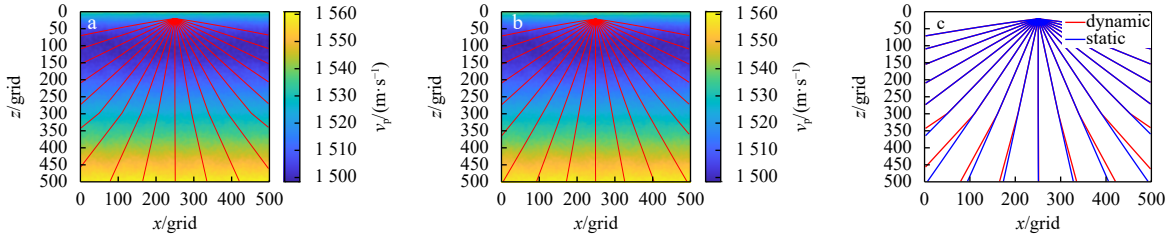

Fig. 17. Travel time calculation results and contrast (deviation is [–1, 1]). a. Static model ray paths; b. dynamic model ray paths; c. comparison of the Static model and dynamic model ray paths. v_p means primary wave velocity.

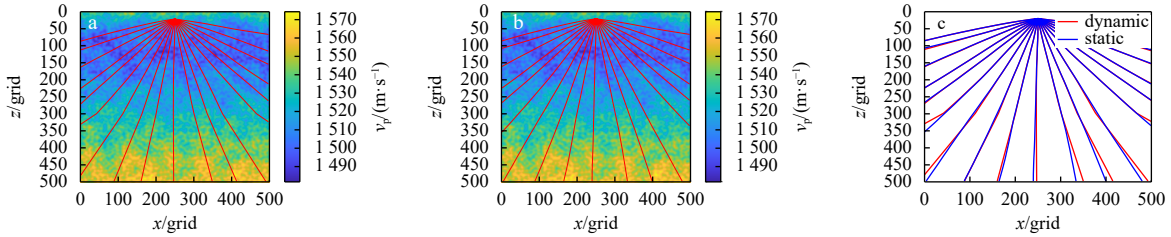

Fig. 18. Travel time calculation results and comparison (deviation is [–10, 10]). a. Static model ray paths; b. dynamic model ray paths; c. comparison of the Static model and dynamic model ray paths. v_p means primary wave velocity.

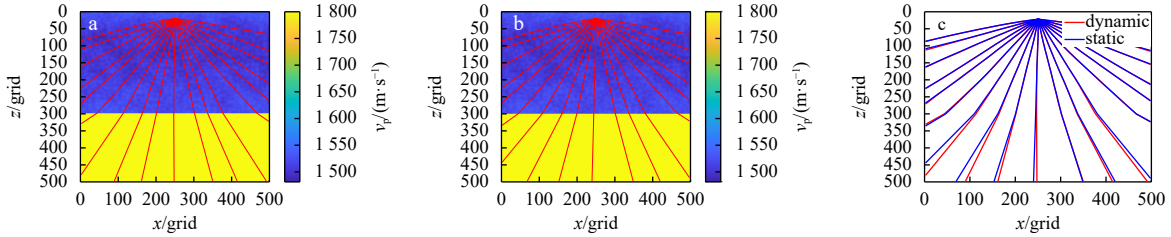

Fig. 19. Ray paths in a two-layer dynamic medium. a. Static model ray paths; b. dynamic model ray paths; c. comparison of the Static model and dynamic model ray paths. v_p means primary wave velocity.

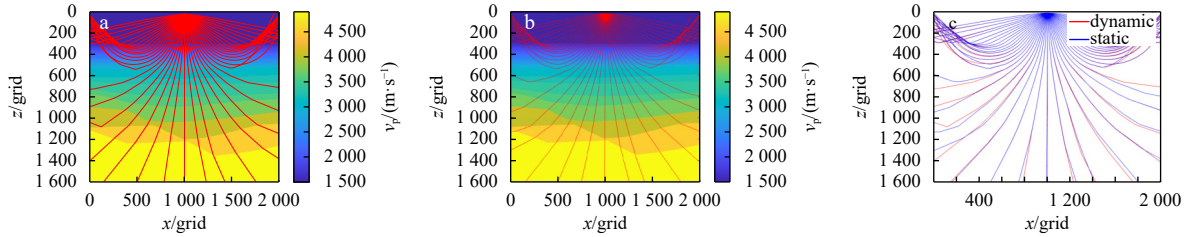

Fig. 20. Ray path in complex dynamic medium. a. Static model ray paths; b. dynamic model ray paths; c. comparison of the Static model and dynamic model ray paths. v_p means primary wave velocity.

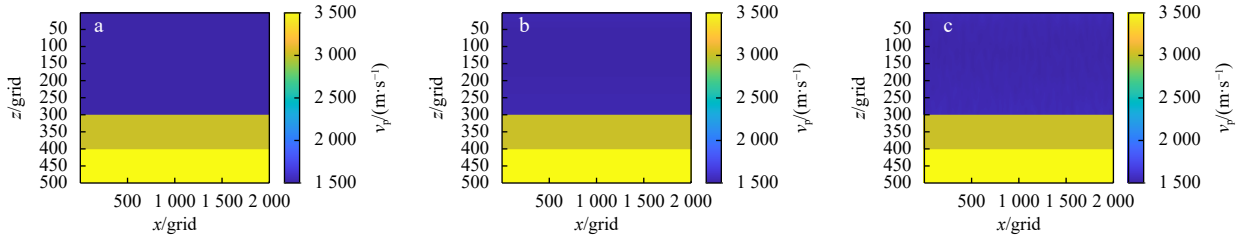

Fig. 21. Horizontal layer model result. a. Horizontal layer model with constant velocity of seawater layer; b. the seawater layer is the horizontal layer model of the Munk model; c. horizontal layer model with seawater layer disturbance [–10, 10]. v_p means primary wave velocity.

larger distortions. Under the undulating interface, a false undulating interface is created. In addition to this, the energy discontinuity is more pronounced on the event axis. And because the calculated ray path is deviated, there will be a lot of messy data on the seabed stratum, which will interfere with the judgment of the normal horizon position.

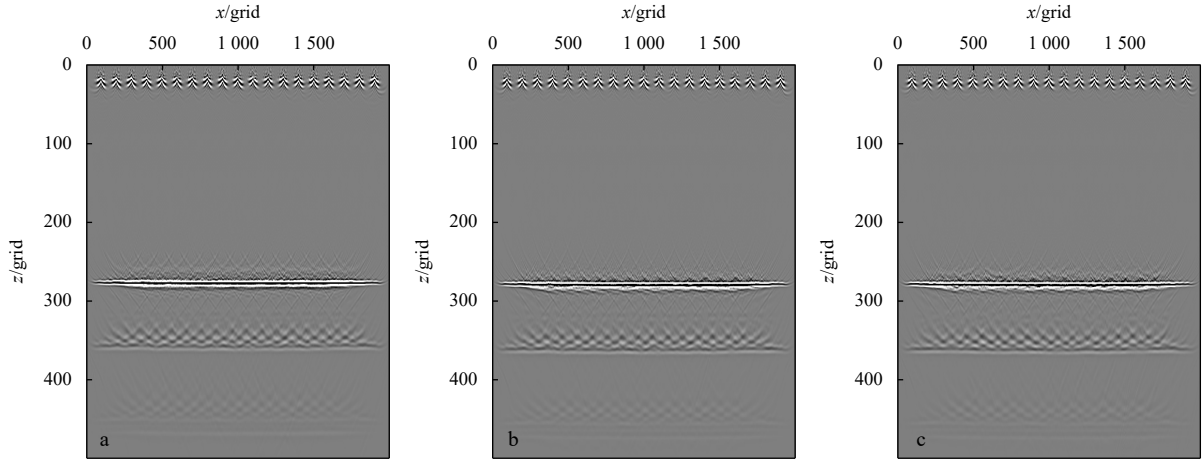

Fig. 22. Gaussian beam imaging results of the horizontal layer model. a. Imaging results of the constant velocity horizontal layer model; b. Munk horizontal layer model imaging results; c. imaging results of random seawater sound velocity model.

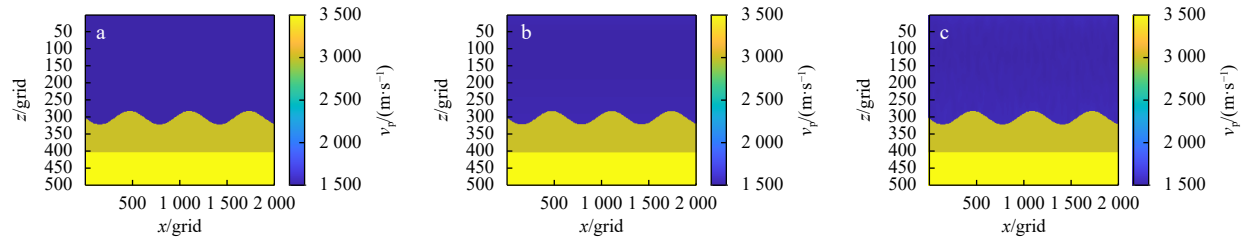

Fig. 23. The undulation model result. a. The fluctuation model of the seawater layer with constant velocity; b. the seawater layer is the undulation model of the Munk model; c. the undulation model with seawater layer perturbation as [–10, 10]. v_p means primary wave velocity.

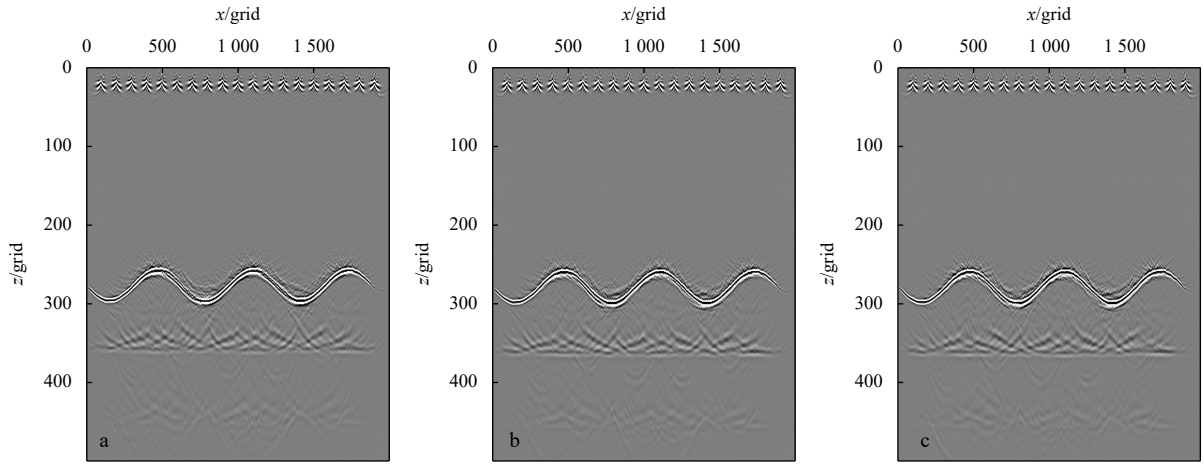

Fig. 24. Gaussian beam imaging results of undulation model. a. Imaging results of constant velocity fluctuation model; b. imaging results of the Munk undulation model; c. imaging results of random seawater sound velocity fluctuation model.

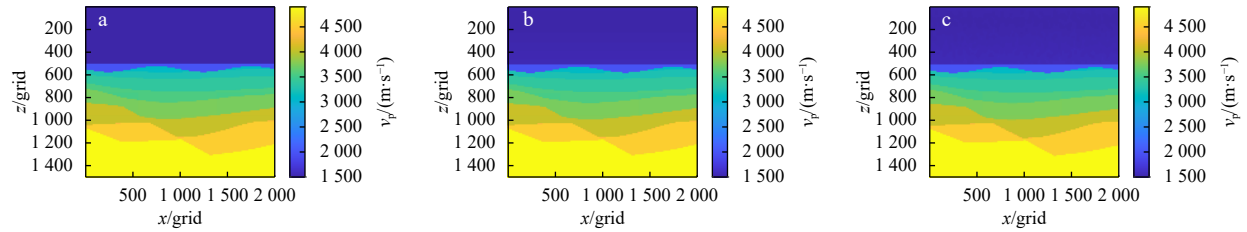

Fig. 25. Complex model result. a. Complex model with constant velocity of seawater layer; b. the seawater layer is a complex model of the Munk model; c. complex model with seawater layer perturbation as [–10, 10]. v_p means primary wave velocity.

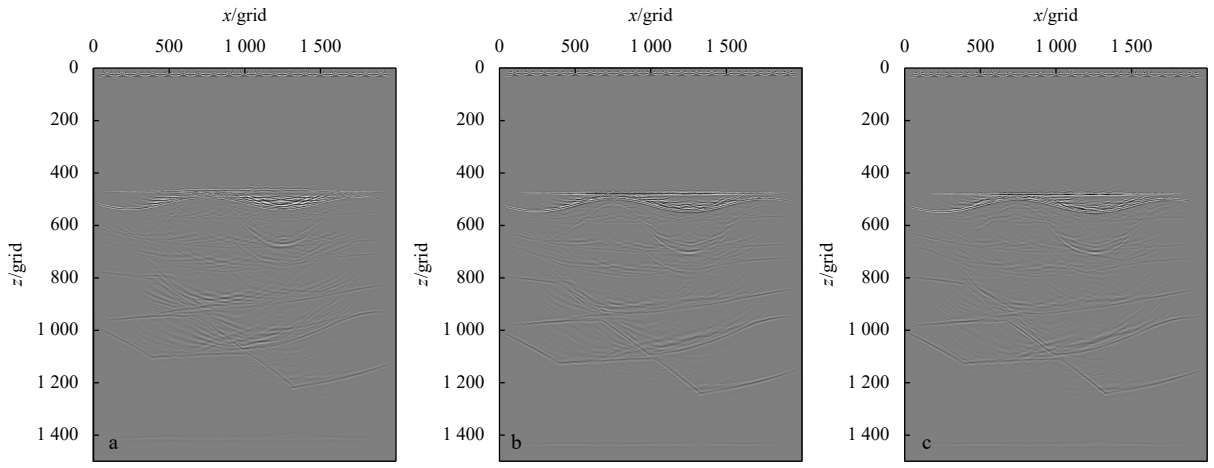

Fig. 26. Gaussian beam imaging result of complex model. a. Imaging results of constant velocity complex model; b. imaging results of the Munk complex model; c. imaging results of complex model of random seawater sound velocity.

5 Conclusions

This paper presents a novel method to generate static or dynamic random velocity models of seawater by combining the Munk model and Perlin noise. The method allows for the generation of continuous, random, and dynamic seawater sound velocity and enables the revelation of the velocity distribution at different scales through noise layering adjustments.

Building on this approach, this paper discusses the applicability of the model in relation to travel time error, ray path, and imaging effect. The method proposed in this paper is suitable for generating static or dynamic seawater velocity models at different scales, providing valuable data support for theoretical seismic forward modeling. However, when using this model to calculate travel time and ray path, there is a notable difference between the calculation using only the Munk model and the calculation using the stochastic seawater velocity model proposed in this paper. Furthermore, the difference between static and dynamic seawater ray paths cannot always be considered negligible. As a consequence of these discrepancies, the event in the imaging results may be distorted to a certain extent, leading to potential challenges for geological interpretation researchers.

Regarding the calculation results of the ray path of the dynamic and static seawater random velocity model, it is essential to consider the influence of seawater dynamics or randomness. Specifically, if the random deviation of seawater sound velocity is small, the influence of seawater dynamics or randomness will be minimal, and analysis may be carried out directly according to the exploration data. However, when this deviation increases, the error caused by the distortion of the ray path cannot be ignored. The imaging results of the static random seawater sound velocity model indicate that the primary effects of inhomogeneous seawater are the discontinuity of the energy axis, the random disturbance of the energy near the axis, and the generation of false horizons. Consequently, it is necessary to take into account several factors such as sea surface fluctuations, deep ocean currents, and others, in addition to the random disturbance of seawater when considering seawater. This highlights the importance of developing a correction method based on the forward modeling results.

References

da Silva Ritter G L. 2010. Water velocity estimation using inversion methods. Geophysics, 75(1): U1–U8, doi: 10.1190/1.3280232

Han Fuxing, Sun Jianguo, Wang Kun, et al. 2015. Analysis of the influence of sea velocity difference on migration imaging in middle and deep layers. Chinese Journal of Geophysics (in Chinese), 58(9): 3439–3447

Holliger K, Levander A. 1994. Seismic structure of gneissic/granitic upper crust: geological and petrophysical evidence from the Strona-Ceneri Zone (northern Italy) and implications for crustal seismic exploration. Geophysical Journal International, 119(2): 497–510, doi: 10.1111/j.1365-246X.1994.tb00137.x

Holliger K, Levander A, Carbonell R, et al. 1994. Some attributes of wavefields scattered from Ivrea-type lower crust. Tectonophysics, 232(1–4): 267–279., doi: 10.1016/0040-1951(94)90089-2

Ikelle L T, Yung S K, Daube F. 1993. 2-D random media with ellipsoidal autocorrelation function. Geophysics, 58(9): 1359–1372, doi: 10.1190/1.1443518

Korn M. 1993. Seismic waves in random media. Journal of Applied Geophysics, 29(3–4): 247–269, doi: 10.1016/0926-9851(93)90007-L

Mackay S, Fried J, Carvill C. 2003. The impact of water-velocity variations on deep water seismic data. The Leading Edge, 22(4): 344–350, doi: 10.1190/1.1572088

Munk W H. 1974. Sound channel in an exponentially stratified ocean, with application to SOFAR. The Journal of the Acoustical Society of America, 55(2): 220–226, doi: 10.1121/1.1914492

Perlin K. 1985. An image synthesizer. ACM SIGGRAPH Computer Graphics, 19(3): 287–296, doi: 10.1145/325165.325247

Qi Peng. 2015. Seismic wave modeling under the complex marine conditions (in Chinese)[dissertation]. Changchun: Jilin University, 9–14

Sun Jianguo. 2021. Inversion of the deep sea water velocity by using Munk formula and seabed reflection travel time. Journal of Jilin University: Earth Science Edition (in Chinese), 51(1): 1–12

Sun Hui, Sun Jianguo, Sun Zhangqing, et al. 2017. Joint 3D traveltime calculation based on fast marching method and wavefront construction. Applied Geophysics, 14(1): 56–63, doi: 10.1007/s11770-017-0611-3

Wang Guangwen, Wang Haiyan, Li Hongqiang, et al. 2021. Research and application of seismic forward simulation technology in deep reflection seismic profile detection. Geophysical and Geochemical Exploration (in Chinese), 45(4): 970–980

Wang Wenfeng, Yue Dali, Zhao Jiyong, et al. 2020. Research on stratigraphic structure based on seismic forward modeling: a case study of the third member of the Yanchang Formation in Heshui area, Ordos Basin. Oil Geophysical Prospecting (in Chinese), 55(2): 411–418

Wei Puli. 2021. Research on methods of velocity modeling for deep seawater (in Chinese)[dissertation]. Changchun: Jilin University, 2–10

Xi Xian, Yao Yao. 2001. 2-D random media and wave equation forward modeling. Oil Geophysical Prospecting (in Chinese), 36(5): 546–552

Yong Fan, Liu Zilong, Ou Yang, et al. 2021. Application of statistical analysis based on random medium model in deep seismic reflection data. Progress in Geophysics (in Chinese), 36(3): 993–1007